Check for updates

Original Article

Design, Optimization, and Characterization of Nilotinib-loaded Supersaturable Self-nanoemulsifying Drug Delivery Systems for Improved Anticancer Efficacy

Journal of Applied Pharmaceutical Science
16(10) 1171–1183, 2026
© The Author(s) 2026
Article reuse guidelines:
in.sagepub.com/journals-permissions-india
DOI: 10.1177/22313354261472048
journals.sagepub.com/home/phs
Sage

Vyshali Parigela[1] and Vijayalakshmi Arumugam[2]

Abstract

Nilotinib is a weakly basic, BCS Class II tyrosine kinase inhibitor with poor aqueous solubility, which may limit its oral bioavailability, particularly at higher gastrointestinal pH. In the present study, a supersaturable self-nanoemulsifying drug delivery system (sSNEDDS) was systematically developed using castor oil, Kolliphor® EL, and propylene glycol, selected based on solubility studies and optimized using a Box–Behnken design. The optimized sSNEDDS exhibited an entrapment efficiency of 87.23%, an average droplet size of 105.87 nm, and a low polydispersity index of 0.069, with an overall desirability value of 1.0. FTIR, XRPD, and DSC studies indicated the absence of significant chemical incompatibility and the transformation of nilotinib toward an amorphous/molecularly dispersed state within the formulation. The optimized sSNEDDS demonstrated satisfactory physical and thermodynamic stability during six months of storage. HPMC K4M was incorporated as a precipitation inhibitor to maintain supersaturation and minimize drug precipitation. In vitro dissolution studies demonstrated greater than 90% drug release within 720 min, representing a substantial improvement compared with conventional SNEDDS and pure nilotinib. The release kinetics followed the Korsmeyer–Peppas model, with an anomalous (non-Fickian) release mechanism. Overall, the developed sSNEDDS improved the solubilization and dissolution performance of nilotinib and demonstrated potential as an oral delivery system for enhancing its bioavailability and therapeutic efficacy.

Keywords

Nilotinib, SNEDDS, precipitation inhibitor, oral bioavailability, Box–Behnken design, nanoemulsion, dissolution enhancement

Received 14 December 2025; **accepted** 13 April 2026

Introduction

Nilotinib is a second-generation tyrosine kinase inhibitor designed to address resistance and intolerance observed with first-generation agents such as imatinib.[1] It primarily manages chronic myeloid leukemia (CML) during the chronic and accelerated phases, particularly in patients expressing the BCR–ABL fusion gene generated by the Philadelphia chromosome translocation.[2,3] Structurally, nilotinib is a synthetic small-molecule inhibitor characterized by a substituted phenyl ring with a trifluoromethyl group, a pyrimidine–pyridine moiety essential for kinase binding, and a methyl-imidazole ring that enhances selectivity toward the ATP-binding site of BCR–ABL TK.[4,5] Despite its potent anticancer activity, nilotinib is practically insoluble in water and exhibits pronounced pH-dependent solubility, with higher solubility

[1] School of Pharmaceutical Sciences, Vels Institute of Science, Technology and Advanced Studies, Chennai, Tamil Nadu, India
[2] Department of Pharmacognosy, School of Pharmaceutical Sciences, Vels Institute of Science Technology and Advanced Studies, Chennai, Tamil Nadu, India

Corresponding author:
Vijayalakshmi Arumugam, Department of Pharmacognosy, School of Pharmaceutical Sciences, Vels Institute of Science Technology and Advanced Studies, Chennai, Tamil Nadu, India.
E-mail: vlakshmi.sps@vistas.ac.in

Creative Commons Non Commercial CC BY-NC: This article is distributed under the terms of the Creative Commons Attribution-NonCommercial 4.0 License (http://www.creativecommons.org/licenses/by-nc/4.0/) which permits non-Commercial use, reproduction and distribution of the work without further permission provided the original work is attributed as specified on the Sage and Open Access pages (https://us.sagepub.com/en-us/nam/open-access-at-sage).

under acidic conditions that markedly decrease at intestinal pH. This behavior leads to variable dissolution and absorption following oral administration, posing significant formulation challenges.[6–8] Pharmacokinetically, nilotinib is administered orally and reaches peak plasma concentrations approximately 3 h post-dose under fasting conditions. Its bioavailability is highly influenced by food intake; high-fat meals substantially increase systemic exposure, necessitating administration on an empty stomach. The drug shows extensive plasma protein binding, is primarily metabolized by CYP3A4, and is a substrate for efflux transporters such as P-glycoprotein and BCRP, which further limit intestinal absorption and contribute to interpatient variability in drug exposure.[6,9–13] Mechanistically, nilotinib selectively fixes to the inactive conformation of BCR–ABL kinase with higher attraction than imatinib and retains activity against several imatinib-resistant mutants, except T315I. By inhibiting BCR–ABL signaling, nilotinib suppresses critical downstream pathways tangled in leukemic cell proliferation and survival—together with RAS/RAF/MEK/ERK, PI3K/AKT, and JAK/STAT—thereby promoting apoptosis and contributing to disease remission in patients with CML.[14–16] However, as a BCS Class II molecule, nilotinib shows low water solubility and dissolution-limited absorption, which remain significant challenges to achieving optimal oral bioavailability. These limitations, combined with efflux-mediated transport, necessitate the development of advanced delivery strategies.[17–19]

Self-nanoemulsifying drug delivery systems (SNEDDS) offer a promising strategy; they automatically generate o/w nanoemulsions in gastrointestinal fluids, thereby enhancing drug solubilization, dissolution rate, and intestinal absorption.[20,21] Additionally, SNEDDS may promote lymphatic uptake and reduce first-pass metabolism, offering a viable platform to improve the pharmacokinetic performance and therapeutic consistency of nilotinib. Despite the proven ability of SNEDDS to enhance the apparent solubility and dissolution of poorly water-soluble drugs, their clinical translation is often compromised by rapid drug precipitation upon dilution in gastrointestinal fluids. This limitation is particularly critical for weakly basic, BCS Class II drugs such as nilotinib, which exhibit pH-dependent solubility and a high tendency to recrystallize under intestinal conditions. To address this challenge, supersaturable SNEDDS (sSNEDDS) have emerged as an advanced formulation strategy, wherein precipitation inhibitors are incorporated to generate and maintain a transient supersaturated state following oral administration.[21]

In contrast to conventional SNEDDS, which rely primarily on drug solubilization, sSNEDDS are specifically designed to delay drug precipitation by inhibiting nucleation and crystal growth, thereby maintaining drug supersaturation and enhancing oral absorption. Although supersaturating drug delivery systems for nilotinib have previously been reported, comprehensive development of a nilotinib-loaded sSNEDDS involving systematic excipient selection, statistical optimization using a Box–Behnken design (BBD), and mechanistic evaluation of precipitation inhibition has been limited. Therefore, the present study focused on the development and optimization of a nilotinib-loaded sSNEDDS using a Quality by Design approach. The formulation strategy incorporated rational excipient selection, precipitation inhibitor screening, optimization of formulation variables, and comprehensive physicochemical characterization, dissolution, stability, and in vitro cytotoxicity evaluations. Collectively, these investigations provide a systematic framework for developing an optimized sSNEDDS and demonstrate its potential as an effective oral lipid-based delivery system for improving the solubility, dissolution, and therapeutic performance of poorly water-soluble anticancer agents such as nilotinib.

Experimental

Chemical and Reagents

Nilotinib was generously supplied by Dr Reddy's Laboratories Limited, India, and all excipients were obtained from SD Fine Chem. Pvt. Ltd. (Mumbai, India). Millipore Milli-Q water was utilized in all experiments, and only analytical-grade chemicals and reagents were employed.

Development of SNEDDS

Selection of SNEDDS Components

Saturation solubility was evaluated using the shake-flask method to systematically screen components (oil, surfactant, and co-surfactant) for the formulation of nilotinib.[22,23] Excess nilotinib was added to 1 g of several vehicles, including oils, surfactants, and co-surfactants, and the blends were vortexed and agitated at 37 °C for 72 h. Post-centrifugation, the supernatant was collected and analyzed by UV spectrophotometry to quantify the drug's solubility. The oil exhibiting the highest solubilization capacity was selected for further screening. Surfactants were then evaluated for emulsification efficiency by mixing equal amounts of the selected oil and surfactant; the number of inversions mandatory for uniform emulsification and percentage transmittance (%T) at 638.2 nm were recorded. Co-surfactants were similarly screened by combining 2:1 (surfactant: co-surfactant) with the selected oil, followed by aqueous dilution and evaluation of emulsification efficiency and transmittance. Based on solubility enhancement, emulsification efficiency, and optical clarity, the optimal concentration of components was selected for SNEDDS formulation development.

Phase Diagram

A pseudo-ternary phase diagram was constructed using a modified visual approach to delineate the self-nanoemulsifying region.[24] Oil, surfactant, and co-surfactant were mixed at

different proportions within the selected experimental ranges of 40–80% w/w oil, 20–60% w/w surfactant, and 0–20% w/w co-surfactant, respectively, while maintaining a total composition of 100% w/w. The mixtures were vortexed to ensure uniform mixing. Subsequently, 100 mg of each mixture was dispersed in 25 mL of distilled water under gentle agitation, and the resulting dispersions were visually evaluated for spontaneous nanoemulsion formation. Clear or slightly bluish, homogeneous dispersions were considered indicative of the self-nanoemulsifying region and were subsequently characterized for droplet size. Formulations producing droplet sizes below 200 nm were considered suitable for further formulation development. All experiments were performed in triplicate, and the phase-diagram results were used to identify suitable and intermediate levels of oil, surfactant, and co-surfactant for subsequent optimization studies.

Experimental Design-based development of SNEDDS

A three-factor, three-level Box–Behnken design (BBD) was employed to systematically optimize the liquid SNEDDS and evaluate the effects of the selected formulation variables. The BBD enables efficient modelling of quadratic response surfaces and assessment of the linear, interaction, and quadratic effects of formulation factors on the selected responses.[25,26] A total of 17 experimental runs, including five centre-point replicates, were generated by systematically varying the levels of Castor oil (A), Kolliphor® EL (B), and Propylene glycol (C) at −1, 0, and +1 coded levels while maintaining a constant drug content. Based on the ternary phase-diagram studies, the selected experimental levels were 46–62 parts of Castor oil, 22–30 parts of Kolliphor® EL, and 16–24 parts of Propylene glycol. The formulation performance was evaluated using droplet size (Y_1), polydispersity index (PDI; Y_2), and entrapment efficiency (EE%; Y_3) as the response variables. The experimental design enabled assessment of the relationships between the formulation factors and the measured responses and facilitated identification of the optimized SNEDDS composition. Design-Expert® software (version 13.0.5.0, Stat-Ease Inc., USA) was used to generate the BBD matrix and perform the response-surface and statistical analyses.[27]

The model was refined using backward elimination to exclude non-significant terms and enhance the fit of the quadratic equation. Model adequacy and reliability were evaluated using ANOVA, lack of fit tests, and the coefficient of determination (R^2) in Design-Expert software, with $p < .05$ as the significance level. The regression coefficients provided insights into the magnitude and direction (synergistic or antagonistic) of each factor's effect. The finalized models were depicted using response surface plots (3D), perturbation plots, and contour plots (2D) to clearly illustrate the effects of formulation variables on the measured results. Multi-response optimization was achieved using a desirability function approach (Derringer and Suich method), in which individual responses were transformed into desirability values (0–1) based on defined maximization or minimization goals, and the desirability values were combined into an overall desirability index using a geometric mean to identify the optimal formulation conditions.[27]

Preparation of Plain and Nilotinib-loaded SNEDDS

Both the placebo (plain) and nilotinib-loaded SNEDDS formulations were meticulously prepared using castor oil, Kolliphor® EL, and propylene glycol in optimized concentrations. For the nilotinib-loaded SNEDDS, accurately measured amounts of the drug were dissolved in the calibrated mixture. In both cases, thorough integration was achieved through a synergistic combination of stirring, vortexing, and controlled heating (37 °C) with a magnetic stirrer, ensuring uniform homogenization of all components. Following complete solubilization, the formulations were stored at room temperature, establishing a robust foundation for subsequent analyses and confirming the precision and reproducibility of the formulation process.[28,29]

Development of sSNEDDS-selection of Precipitation Inhibitor and Preparation of sSNEDDS

To maintain drug supersaturation and inhibit precipitation following dilution, an in vitro precipitation study was conducted using different polymeric precipitation inhibitors, including hydroxypropyl methylcellulose (HPMC) K4M, polyvinylpyrrolidone (PVP K30), Poloxamer 407, and Eudragit® L100. The optimized SNEDDS containing each polymer was dispersed in 100 mL of simulated gastric fluid (SGF, pH 1.2) maintained at 37 °C ± 0.5 °C under continuous stirring at 100 rpm to simulate gastric conditions. At predetermined time intervals (5, 15, 30, 45, 60, 90, 120, 180, and 240 min), 1 mL aliquots were withdrawn and immediately centrifuged at 12,000 × g for 5 min to separate any precipitated drug. The resulting supernatant was collected, appropriately diluted with methanol to dissolve the remaining drug, and analyzed using UV–Visible spectrophotometry to determine the concentration of dissolved nilotinib over time, thereby evaluating the precipitation-inhibiting ability of each polymer.[29,30]

Based on the precipitation inhibition study, HPMC K4M was selected as the most effective polymer. The sSNEDDS was prepared by incorporating 2.0% (w/w) HPMC K4M into the optimized SNEDDS. The formulation was vortex-mixed for 5 min to ensure uniform polymer dispersion and subsequently equilibrated in a water bath maintained at 37 °C ± 0.5 °C for 24 h before further physicochemical characterization and performance evaluation.[31]

Comprehensive Physicochemical Characterization

The physicochemical attributes of both nilotinib and the SNEDDS formulation were meticulously examined through various analytical techniques.

Determination of Size Distribution and Surface Charge

Droplet size dispersion and surface charge (zeta potential) of the formulations were measured after a 100-fold dilution with deionized water, followed by gentle mixing to achieve uniform dispersion. Dynamic light scattering analyses were performed using a Mastersizer 2000 (Malvern Instruments, UK) at a fixed scattering angle of 90°, with zeta potential measured via an integrated electrode system. All measurements were conducted in triplicate, and average droplet size and PDI were reported to ensure a reliable assessment of formulation stability.

Surface Morphology Analysis

The droplet morphology of the optimized nilotinib-loaded SNEDDS was analyzed using a JEOL JEM 2100F transmission electron microscope (USA). The formulation was first diluted 1000-fold with distilled water, applied onto a carbon-coated grid, and marked with 2% uranyl acetate. Imaging was performed at 200 kV with a camera length of 100 cm to visualize nanoscale droplet structures.

FTIR, DSC, and XRPD Analysis

Fourier Transform Infrared Spectroscopy (FTIR), differential scanning calorimetry (DSC), and powder X-ray diffraction (PXRD) analyses were conducted to examine the chemical compatibility, thermal properties, and solid-state characteristics of nilotinib and the SNEDDS formulations. FTIR spectra were recorded using the KBr pellet procedure on a Shimadzu FTIR-8400S spectrophotometer over a series of 400–4000 cm^{-1} to identify potential interactions between formulation components. The thermal strategy was investigated by DSC on a PerkinElmer DSC/7, standardized using indium. Around 5 mg of each sample was placed in aluminum pans and heated (30 °C–400 °C) at 10 °C per min under a nitrogen atmosphere, with a blank pan serving as reference. The solid-state form of the drug—crystalline or amorphous—was assessed using PXRD on a Bruker D8 Advance diffractometer, scanning from 10° to 80° 2θ at a rate of 5°/min under ambient conditions.

RI Measurement

The isotropic nature of nilotinib-loaded SNEDDS and sSNEDDS was evaluated by measuring the refractive index (RI). A 1000-fold dilution of each formulation was prepared with distilled water, and a single drop was analyzed at room temperature using an Abbe-type refractometer. To ensure precision, measurements were executed in triplicate, and the average values were recorded to ensure a reliable assessment of the isotropic properties.

Evaluation of Optical Clarity and %T

The %T of nilotinib-loaded SNEDDS and sSNEDDS, indicating optical clarity, was measured at 650 nm by a double-beam UV spectrophotometer using water as a blank solution. A 1000-fold dilution of each formulation was prepared using distilled water, then transferred to a stoppered volumetric flask and left undisturbed for 2 h before measurement. To ensure an accurate assessment of formulation transparency, average values were recorded after repeating the procedure three times.

Drug Assay

The amount of drug present in SNEDDS and sSNEDDS formulations was quantified spectrophotometrically at 260 nm. An accurately weighed sample was liquefied in 10 mL of methanol and vortexed for 10 min to achieve complete solubilization. The resultant solution was filtered (0.45 µm membrane) and analyzed against a blank to ensure accurate measurement. The assay was conducted on three separate samples, and the mean values were recorded to ensure reliability and precision.

Drug Release Kinetics

The in vitro release of nilotinib from the SNEDDS and sSNEDDS formulations was evaluated using a USP Type II (paddle) dissolution apparatus (Electrolab, TDL-08). An accurately weighed quantity of each formulation (420 mg) was dispersed in 500 mL of SGF (pH 1.2) maintained at 37 °C ± 0.5 °C, with the paddle rotation speed set at 50 rpm. Aliquots of 5 mL were withdrawn at predetermined time intervals of 5, 10, 15, 30, 45, 60, 90, and 120 min, and an equal volume of fresh dissolution medium maintained at the same temperature was added after each sampling to maintain a constant volume. After 120 min, the dissolution medium was adjusted to pH 6.8 by adding 250 mL of 0.3 M dibasic sodium phosphate, resulting in a total dissolution volume of 750 mL to simulate intestinal conditions. Dissolution sampling was continued at 180, 240, 360, 480, 600, and 720 min. At each sampling point, 5 mL of the dissolution medium was withdrawn, filtered, appropriately diluted, and analyzed by UV–Visible spectrophotometry to determine the nilotinib concentration. The withdrawn volume was replaced with an equal volume of fresh pH 6.8 dissolution medium maintained at 37 °C ± 0.5 °C, and cumulative drug release was calculated after correcting for sample withdrawal and medium replacement. All dissolution studies were performed in triplicate (n = 3). The release profiles were fitted to zero-order, first-order, Higuchi, and Korsmeyer–Peppas kinetic models to evaluate the drug release kinetics and mechanism.

Stability Evaluation

Stability of SNEDDS and sSNEDDS formulations was comprehensively assessed through thermodynamic, gastrointestinal, dilution, and accelerated stability studies. Thermodynamic stability was examined by exposing the formulations to six cycles of alternating heating (40 °C) and cooling (4 °C), followed by freeze–thaw cycles (−21 °C–25 °C for 48 h) and centrifugation at 3500 rpm for 30 min to detect phase parting; formulations that rapidly returned to their original state were deemed stable. Gastrointestinal stability was evaluated by incubating the formulations in SGF for 2 h, followed by sim-

ulated intestinal fluid (SIF, pH 6.8) for 6 h, after which droplet size and PDI were evaluated to monitor precipitation. Dilution robustness was tested by diluting the formulations 200-, 400-, 600-, and 800-fold in SGF, incubating at 37 °C for 2 h, and subsequently assessing droplet size and PDI. Accelerated stability studies were conducted at 40 °C/75% RH for a period of 3 months, whereas long-term stability studies were performed at 4 °C and 25 °C for up to 6 months

Cytotoxicity and Antiproliferative Assessment Using MTT Assay

The cytotoxicity of the nilotinib-loaded SNEDDS and sSNEDDS formulations was evaluated using the human chronic myelogenous leukemia cell line (K562) by the MTT assay with minor modifications to a previously reported method.[30] K562 cells were cultured in complete growth medium and seeded into 96-well plates at a density of 2×10^4 cells/well in 200 µL of culture medium. As K562 cells are suspension cells, the seeded cells were incubated at 37 °C ± 1 °C in a humidified atmosphere containing 5% ± 1% CO_2 for 24 h before treatment. The cells were subsequently treated with various concentrations of the nilotinib-loaded formulations and incubated for an additional 48 h under identical culture conditions. Untreated cells served as the negative control, whereas blank SNEDDS (drug-free formulation) was used as the vehicle control.

Following the treatment period, 100 µL of MTT solution (0.5 mg/mL) was added to each well, and the plates were incubated for 3 h to allow the formation of formazan crystals. The crystals were dissolved in dimethyl sulfoxide, and the absorbance was measured at 570 nm using a microplate reader. All experiments were performed in triplicate ($n = 3$), and cell viability was expressed as a percentage relative to the untreated control. Dose–response curves were generated by plotting the percentage of cell viability against the drug concentration, and the IC_{50} values were determined by nonlinear regression analysis using an appropriate curve-fitting model. Cell viability (%) was calculated using Equation (1).

$$\% \text{ Viability} = \frac{\text{Absorbance of treated cellls}}{\text{Absorbance of control cellls}} \times 100 \quad (1)$$

Where:

Absorbance of treated cells is measured as optical density (OD) at 570 nm for cells exposed to the test formulation.

Absorbance of control cells refers to the OD recorded at 570 nm for untreated cells (negative control), which is considered 100% viable.

Statistical Evaluation

All data are articulated as mean ± SD. Statistical studies were conducted to assess variations among the formulations. One-way ANOVA was used to assess overall variation, while pairwise comparisons between specific groups were performed using Student's t test. Statistical significance was assessed using $p < .05$, ensuring the results' reliability and robustness.

Results and Discussion

Solubility screening represents a fundamental step in SNEDDS development, as drug solubilization within formulation excipients governs drug loading, self-emulsification behavior, and the risk of precipitation upon gastrointestinal dilution. Owing to the low aqueous solubility of nilotinib, its solubility was assessed across a range of oils, surfactants, and co-surfactants to identify appropriate excipients capable of forming a stable nanoemulsion with an extensive self-emulsifying region. Among the oils evaluated, castor oil demonstrated the highest solubility for nilotinib, making it the most suitable oil phase, whereas linseed oil showed the lowest solubility. Non-ionic surfactants demonstrated superior solubility profiles, with Kolliphor® RH 40 and Kolliphor® EL showing the highest drug solubilization, followed by Tween-80. Among co-surfactants, PEG-600, Carbitol, and propylene glycol exhibited appreciable solubilizing ability. These findings provided a rational basis for excipient selection, while also emphasizing that solubility alone must be complemented by efficient emulsification and favorable phase behavior.

Based on emulsification efficiency and compatibility with castor oil, Kolliphor® EL was chosen as the surfactant due to its high hydrophilic–lipophilic balance, strong self-emulsifying ability, and excellent transparency upon dilution. Co-surfactant screening with Kolliphor® EL identified propylene glycol as the most effective co-surfactant, producing clear emulsions with minimal flask inversions and superior stability. Overall, the comprehensive solubility and emulsification studies guided the selection of castor oil, Kolliphor® EL, and propylene glycol as the optimal oil, surfactant, and co-surfactant, respectively, providing a strong basis for the development of an optimized nilotinib SNEDDS formulation.

The ternary phase diagrams were generated to determine optimal proportions of oil, surfactant, and co-surfactant required to form stable nanoemulsions upon aqueous dilution. Based on prior solubility and emulsification studies, castor oil, Kolliphor® EL, and propylene glycol were designated as the oil, surfactant, and co-surfactant, respectively. Various combinations were prepared and titrated with water, and the resulting dispersions were visually evaluated. Clear or slightly bluish transparent systems were considered successful nanoemulsions and mapped within the phase diagram.

The shaded region in the diagram (Figure 1) represents the self-nanoemulsifying zone, where fine oil-in-water nanoemulsions with droplet sizes below 200 nm were consistently formed. Increasing the surfactant-to-co-surfactant ratio broadened the nanoemulsion region, likely due to improved interfacial stabilization and reduced surface tension. Based on these observations, the optimized formulation space was defined as 46%–62% castor oil, 22%–30% Kolliphor® EL, and 16%–24% propylene glycol, providing a robust compositional range for further optimization and drug loading.

SNEDDS optimization was carried out using a 33BBD to investigate the effects of castor oil (*A*), Kolliphor® EL (*B*), and propylene glycol (*C*) on droplet size (Y_1), PDI (Y_2), and EE% (Y_3). The factors were varied within predefined ranges (*A*: 46%–62%, *B*: 22%–30%, *C*: 16%–24%), based on the nanoemulsification region identified from ternary phase diagrams. Seventeen trials were generated using Design-Expert® software (v13.0.5.0). Data were analyzed by multiple linear regression and ANOVA, and the effects of formulation variables were interpreted using regression equations and 3-D response surface plots to identify the optimized SNEDDS composition.[30,31]

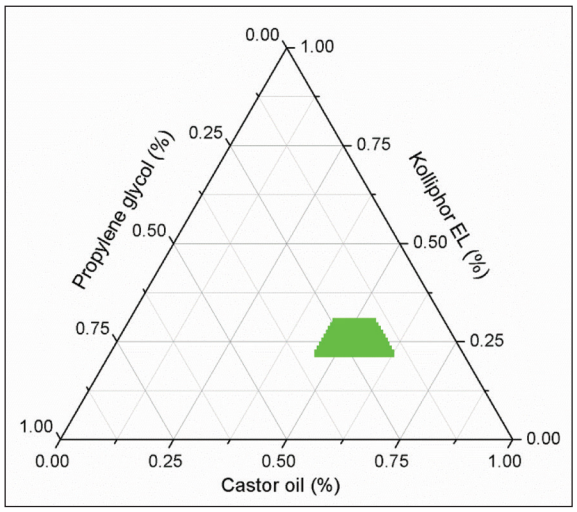

Figure 1. Optimization Through Experimental Design.

Droplet Size

Droplet size is an important determinant of SNEDDS performance because it can influence drug solubilization, interfacial surface area, dispersion, and dissolution. In the present study, the nilotinib-loaded SNEDDS formulations exhibited droplet sizes ranging from 76.54 to 185.68 nm across the 17 experimental runs, confirming the formation of nano-sized emulsions. A quadratic model effectively captured the effects of castor oil (*A*), Kolliphor® EL (*B*), and propylene glycol (*C*) on droplet size, showing excellent agreement between predicted and experimental values and demonstrating high model reliability.

Statistical analysis demonstrated high model significance ($F = 923.24$, $p < .0001$), non-significant lack of fit ($p > .05$), and strong analytical power (predicted $R^2 = 0.9947$, adjusted $R^2 = 0.9965$, adequate precision = 104.51). Regression analysis revealed that castor oil increased droplet size (positive linear and quadratic effects), whereas Kolliphor® EL and propylene glycol reduced droplet size (negative linear effects), with Kolliphor® EL exerting the strongest emulsification effect. Quadratic terms indicated that excessive surfactant levels may slightly increase droplet size due to saturation or viscosity effects. Perturbation analysis (Figure 2A) further confirmed that Kolliphor® EL was the

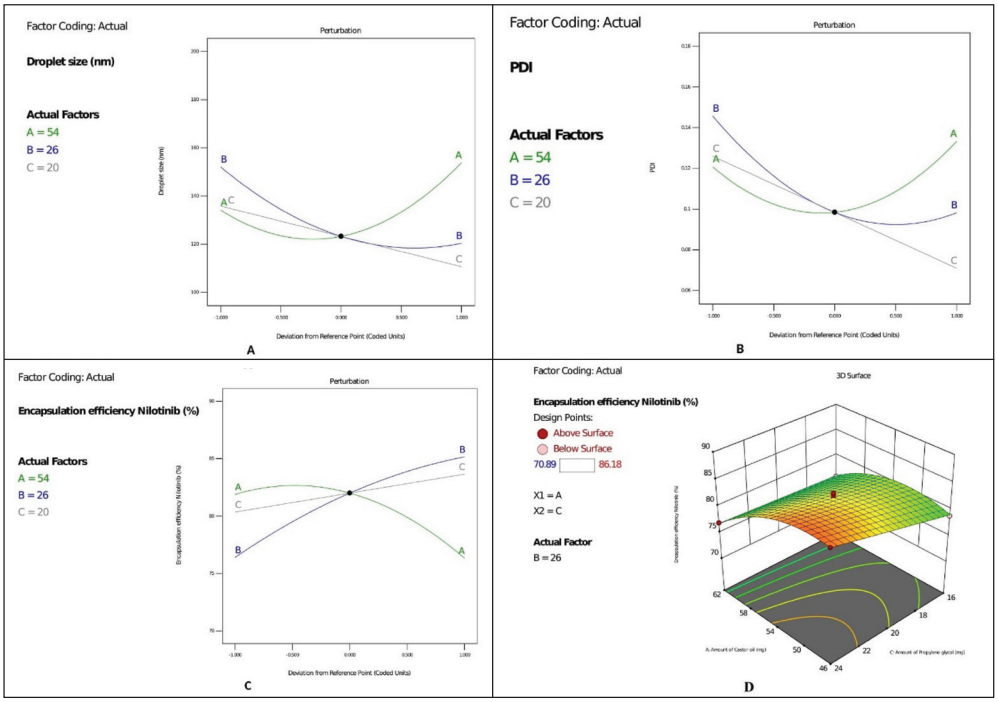

Figure 2. (A) Effects of *A*, *B*, and *C* on Droplet Size (Perturbation Plot), (B) Effects of *A*, *B*, and *C* on PDI (Perturbation Plot), (C) Effects of *A*, *B*, and *C* on Encapsulation Efficiency (Perturbation Plot), and (D). Combined Influence of *A* and *C* at a Fixed Level of B on encapsulation Efficiency (Response Surface Plot).

most influential factor in minimizing droplet size, underscoring the need to balance the optimization of all components to achieve stable, nano-sized emulsions.

Polydispersity Index

PDI is a measure of droplet size uniformity and emulsion stability, ranging from 0.07 to 0.18 for all nilotinib-loaded SNEDDS formulations, remaining well below the acceptable threshold of 0.3 and confirming monodisperse systems. Quadratic model analysis demonstrated that Kolliphor® EL (*B*) and propylene glycol (*C*) significantly reduced PDI, enhancing droplet uniformity, whereas castor oil (*A*) showed a mild increasing effect. The model demonstrated robust statistical validity ($F = 104.18$, $p < .0001$) with a non-significant lack of fit ($p = .9812$) and high predictive accuracy (adjusted $R^2 = 0.9699$, predicted $R^2 = 0.9631$, adequate precision = 32.34). Furthermore, the strong correlation between experimental and predicted PDI values confirmed the reliability of the model. Regression and perturbation analyses (Figure 2B) indicated that increasing surfactant and co-surfactant concentrations improve emulsification efficiency and homogeneity, while excessive oil or surfactant levels may slightly increase PDI due to viscosity or phase effects. Overall, optimized levels of Kolliphor® EL and propylene glycol are critical for achieving uniform, stable SNEDDS formulations.

EE% of Nilotinib

EE% is a key quality attribute of SNEDDS, reflecting the system's ability to retain the drug within nanoemulsion droplets. In this study, EE% of nilotinib ranged from 70.89% to 86.18%, indicating efficient drug entrapment across formulations. Regression analysis revealed that Kolliphor® EL (*B*) and propylene glycol (*C*) exerted significant positive effects on EE%, attributed to improved drug solubilization and interfacial stabilization, whereas castor oil (*A*) showed a mild negative effect, likely due to dilution. The quadratic model for EE% was highly significant ($F = 157.26$, $p < 0.0001$) and demonstrated excellent predictive performance, with an R^2 of 0.9895, adjusted R^2 of 0.9832, and predicted R^2 of 0.9762. The relatively small residual range (−0.89 to +0.85) and adequate precision value of 45.53 further indicated satisfactory model performance. Kolliphor® EL exhibited the strongest positive influence on EE%, followed by Propylene glycol. The quadratic and interaction effects suggested that excessive levels of certain formulation components could adversely affect drug incorporation. The lack-of-fit test was non-significant ($p = 0.84$), while the reported coefficient of variation (CV) was 0.69%, indicating low experimental variability based on the original model analysis. Perturbation and response-surface analyses (Figure 2C and 2D) indicated that higher EE% was associated with appropriate levels of Kolliphor® EL and Propylene glycol and a controlled proportion of Castor oil. Overall, the findings emphasize the importance of optimizing the proportions of oil, surfactant, and co-surfactant to achieve efficient incorporation of nilotinib into the SNEDDS.

Optimization Through Desirability Function

A desirability function approach was employed to simultaneously optimize the critical formulation responses of the nilotinib-loaded SNEDDS, namely droplet size (Y_1), polydispersity index (PDI; Y_2), and entrapment efficiency (EE%; Y_3), with the objectives of minimizing droplet size and PDI while maximizing EE%. Each response was transformed into an individual desirability value ranging from 0 to 1, and the overall desirability was calculated using the geometric mean of the individual desirabilities in Design-Expert® software. The optimized formulation, comprising castor oil, Kolliphor® EL, and propylene glycol at the optimized proportions, yielded predicted values of 105.87 nm for droplet size, 0.069 for PDI, and 87.23% for EE%, with an overall desirability of 1.000. Experimental validation of the optimized formulation demonstrated good agreement with the predicted values, producing droplet sizes ranging from 102.43 to 112.32 nm, a PDI below 0.09, and an EE% of up to 87.86%, thereby confirming the predictive capability and reliability of the optimization model.

Screening for a Precipitation Inhibitor

To develop a sSNEDDS capable of maintaining nilotinib in a supersaturated state, various precipitation inhibitors were screened under non-sink conditions. Poloxamer 407, Eudragit L100, PVP K30, and HPMC K4M (5% w/w of optimized SNEDDS, S1) were evaluated in 100 mL dissolution medium simulating residual gastric volume. Apparent concentration–time profiles (Figure 3) revealed rapid precipitation from SNEDDS without an inhibitor, with drug levels declining to 68 µg/mL at 240 min. In contrast, sSNEDDS formulations significantly delayed precipitation, with HPMC K4M

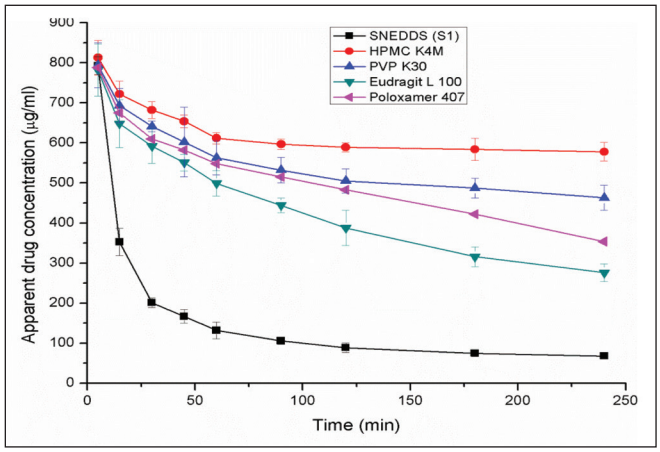

Figure 3. In Vitro Mean Apparent Nilotinib Concentration–Time Profiles Observed from Various Polymer Precipitation Inhibitors.

showing the strongest inhibition, at 813 µg/mL at 5 min and 578 µg/mL at 240 min. PVP K30 demonstrated moderate effectiveness, while Poloxamer 407 and Eudragit L100 showed comparatively lower inhibition. The effect of HPMC K4M concentration (0.5%–5.0% w/w) on supersaturation was further investigated. Precipitation inhibition increased with polymer concentration up to 2.0%, beyond which no significant improvement was observed. Although higher HPMC levels slightly increased emulsification time, all formulations emulsified within 1 min. Based on its superior precipitation inhibition and acceptable emulsification performance, 2.0% w/w HPMC K4M was designated as the optimal precipitation inhibitor for the final sSNEDDS formulation.

Characterization

The in vivo performance and physical stability of SNEDDS and sSNEDDS formulations depend on critical quality attributes such as droplet size, polydispersity index (PDI), and zeta potential. Droplet size can influence drug release, dispersion, and absorption, with smaller droplets providing a greater interfacial surface area. In the present study, the nilotinib-loaded SNEDDS formulations (S1–S3) exhibited droplet sizes ranging from 102.43 to 112.32 nm, whereas the sSNEDDS formulations (F1–F3) showed smaller droplet sizes ranging from 83.64 to 89.58 nm, indicating efficient self-nanoemulsification and good dispersibility. The PDI values ranged from 0.06 to 0.09 across all formulations, indicating relatively narrow droplet-size distributions. The mean zeta-potential values ranged from −18.8 to −26.9 mV for the SNEDDS formulations and from −19.9 to −21.7 mV for the sSNEDDS formulations. These values indicate moderate electrostatic repulsion rather than strong electrostatic stabilization. Therefore, the physical stability of the formulations is likely attributable to a combination of interfacial and steric stabilization provided by the surfactant/co-surfactant system, in addition to the contribution of electrostatic repulsion. Collectively, the results demonstrate the formation of nano-sized formulations with relatively uniform droplet distributions and satisfactory physical characteristics for further evaluation as oral delivery systems for nilotinib. The experimental design and levels of the independent variables employed in the Box–Behnken Design (BBD) are presented in Table 1. The experimental runs generated by the Box–Behnken Design (BBD) along with the observed responses are summarized in Table 2. Detailed results are presented in Table 3. The morphology of the optimized SNEDDS and sSNEDDS formulations was examined using transmission electron microscopy (TEM), and the representative images are shown in Figure 4.

Table 1. BBD Design with Levels of Variables.

	Levels		
Independent Variables	−1	0	+1
A: Quantity of castor oil (% w/w)	46	54	62
B: Quantity of Kolliphor® EL (% w/w)	22	26	30
C: Quantity of propylene glycol (% w/w)	16	20	24
Dependent Variables		Goal	
Y_1: Droplet size in nm		Minimize	
Y_2: PDI		Minimize	
Y_3: Encapsulation (%)		Maximize	

Table 2. BBD with Observed Responses.

Run	A: Oil (parts)	B: Surfactant (parts)	C: Co-surfactant (parts)	Y1: Droplet size (nm)	Y2: PDI	Y3: EE (%)
1	54	30	24	110.38	0.08	84.18
2	54	22	24	135.24	0.12	80.29
3	54	26	20	125.36	0.10	81.12
4	54	26	20	122.43	0.11	82.08
5	54	22	16	160.54	0.16	74.76
6	46	26	16	140.64	0.15	78.84
7	54	26	20	124.79	0.10	81.69
8	54	26	20	122.32	0.09	82.53
9	62	22	20	185.68	0.18	70.89
10	62	26	24	145.53	0.14	77.94
11	54	26	20	123.59	0.09	82.86
12	62	30	20	138.26	0.11	79.39
13	54	30	16	132.72	0.13	83.64
14	46	22	20	172.48	0.19	73.88
15	46	30	20	130.66	0.10	85.65
16	57	30	16	78.12	0.08	86.78
17	57	30	16	76.54	0.17	84.42

Table 3. Droplet Size Distribution, Polydispersity Index, and Zeta Potential Analysis.

Sample	Particle Size Mean ± SD (nm)	Polydispersity Index	Zeta Potential (mV)
S1 (SNEDDS)	112.32 ± 3.54	0.09 ± 0.005	−18.8 ± 3.1
S2 (SNEDDS)	102.43 ± 2.98	0.07 ± 0.005	−23.9 ± 2.3
S3 (SNEDDS)	105.56 ± 4.12	0.06 ± 0.005	−26.9 ± 1.8
F1 (sSNEDDS)	87.82 ± 2.32	0.09 ± 0.005	−19.9 ± 2.2
F2 (sSNEDDS)	83.64 ± 3.12	0.07 ± 0.005	−21.7 ± 1.5
F3 (sSNEDDS)	89.58 ± 2.39	0.06 ± 0.005	−20.6 ± 1.6

Note: All measurements were conducted in triplicate, and the values are presented as mean ± SD (n = 3).

To assess alterations in the solid-state characteristics and possible molecular interactions of nilotinib after incorporation into the sSNEDDS, FTIR, XRPD, and DSC were performed on the pure drug, the physical mixture, and the finalized formulation. FTIR spectra (Figure 5A) of pure nilotinib displayed characteristic functional group peaks, all of which were retained in both the physical mixture and sSNEDDS without substantial shifts or disappearance, demonstrating the absence of chemical interactions with excipients. Minor reductions in peak intensity in the sSNEDDS suggested molecular dispersion of the drug. X-ray Powder Diffraction (XRPD) analysis (Figure 5B) showed

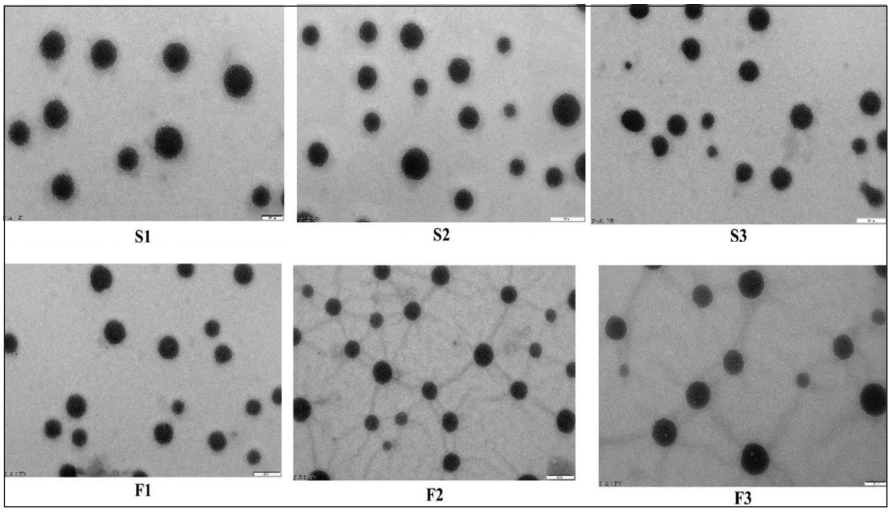

Figure 4. TEM Images of SNEDDS and sSNEDDS Formulations.

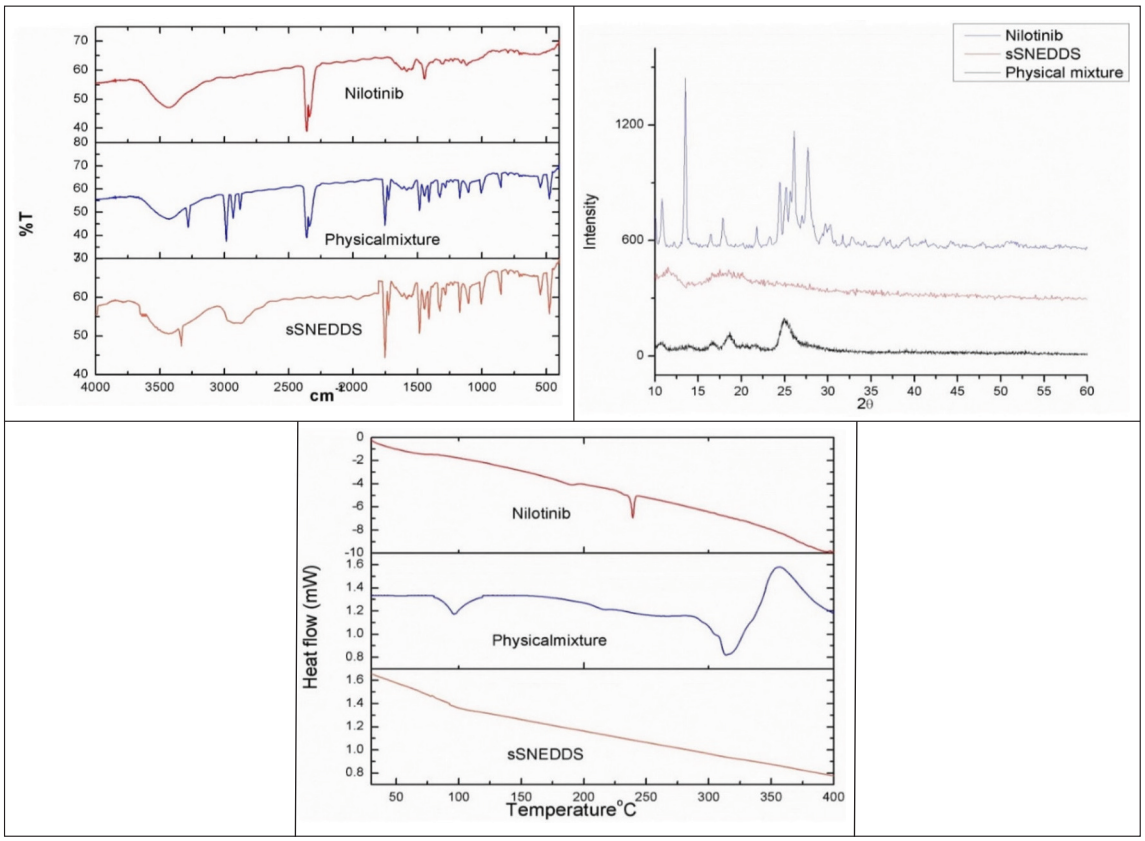

Figure 5. (A) FTIR Spectra of Pure Nilotinib, SNEDDS and sSNEDDS Formulations, (B) XRD Pattern of Pure Nilotinib, SNEDDS and sSNEDDS Formulations, (C) DSC Thermograms of the Drug, Physical Mixture, and sSNEDDS Formulation.

sharp diffraction peaks for pure nilotinib, confirming its crystalline nature, while these peaks were diminished in the physical mixture and completely absent in sSNEDDS, demonstrating conversion to an amorphous form. DSC thermograms (Figure 5C) supported these findings, with the melting endotherm of nilotinib present in the pure drug and physical mixture but absent in the sSNEDDS. Collectively, these results confirm complete amorphization and molecular dispersion of nilotinib within the sSNEDDS, which is advantageous for improving solubility, dissolution, and oral bioavailability.

The RI of nilotinib-loaded sSNEDDS was measured to endorse the isotropic and transparent nature of the formed nanoemulsions. All three batches exhibited consistent RI values of 1.31–1.34, indicating formulation uniformity and optical clarity upon dilution. Complementary transmittance studies further supported these findings, with all batches showing nearly 100% transmittance, confirming the formation of clear, homogeneous, and isotropic nanoemulsions suitable for efficient drug delivery.

The drug release characteristics of pure nilotinib, SNEDDS formulations (S1–S3), and the optimized sSNEDDS (F2) were evaluated in SGF and SIF (Figure 6). Pure nilotinib exhibited poor dissolution, releasing only approximately 12.5% of the drug over 720 min, consistent with its poor aqueous solubility. In contrast, the SNEDDS formulations markedly enhanced drug dissolution, achieving approximately 70%–75% cumulative drug release at 720 min. The optimized sSNEDDS (F2) exhibited the highest dissolution performance, releasing 91.34% ± 2.38% of nilotinib within 720 min, with an initial release of 5.14% ± 0.33% within the first 15 min, indicating rapid self-emulsification and efficient drug dispersion. The enhanced dissolution performance of F2 may be attributed to the formation of nanosized droplets, which provide a large interfacial surface area for drug dissolution, together with the presence of HPMC K4M, which helps maintain supersaturation and minimize drug precipitation. The improved dissolution performance of both SNEDDS and S-SNEDDS formulations, compared with pure nilotinib, was statistically significant ($p < .05$), indicating that the sSNEDDS approach effectively overcomes solubility limitations and has the potential to improve the dissolution behavior and potential oral bioavailability of nilotinib.

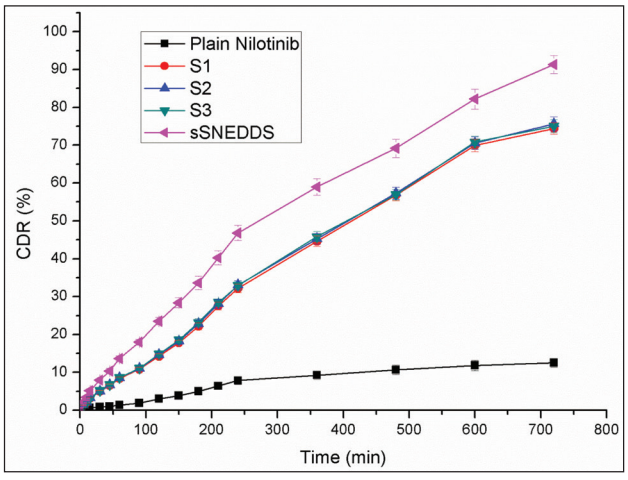

Figure 6. In Vitro Drug Release Profile from SNEDDS and sSNEDDS Formulations.

In vitro drug release data for optimized SNEDDS and sSNEDDS nilotinib were fitted to several kinetic models (Table 4). The Korsmeyer–Peppas model showed the highest goodness-of-fit, with correlation coefficients (R^2) of 0.9948 for SNEDDS and 0.9972 for sSNEDDS. The corresponding release exponent values ($n = 0.8518$ for SNEDDS and 0.7723 for sSNEDDS) were indicative of anomalous (non-Fickian) release behavior, implying that nilotinib release is controlled by a combined contribution of diffusion and matrix erosion processes. Zero-order kinetics also showed good correlation, reflecting a relatively constant release rate, while the Higuchi model indicated that diffusion contributes but is not the sole mechanism. Overall, the results confirm that nilotinib release from both formulations follows anomalous transport, involving both matrix diffusion and structural relaxation.

The optimized nilotinib-loaded SNEDDS formulation (S3) demonstrated excellent thermodynamic stability under various stress conditions. The formulation remained clear and homogeneous, with no evidence of phase separation, drug precipitation, or creaming during heating–cooling cycles (4 °C–40 °C), freeze–thaw cycles (−21 °C–25 °C), and centrifugation at 3500 rpm for 30 min, indicating its robustness against thermal and mechanical stress. Furthermore, long-term stability studies conducted under refrigerated (4 °C ± 1 °C) and ambient (25 °C ± 2 °C) storage conditions for 6 months showed only minor changes in droplet size, zeta potential, and PDI, with no evidence of physicochemical instability (Table 5). Under accelerated storage conditions (40 °C ± 2 °C/75% ± 5% RH), the optimized SNEDDS remained stable throughout the 3-month study period without any significant changes in its physicochemical characteristics. These findings demonstrate that the optimized nilotinib-loaded SNEDDS (S3) possesses excellent physical and thermodynamic stability, supporting its suitability for storage and subsequent development as an oral lipid-based drug delivery system.

The MTT assay results demonstrated a dose-dependent reduction in cell viability for both pure nilotinib and the

Table 4. Drug Release Kinetic Parameters of Nilotinib SNEDDS and sSNEDDS.

Kinetic Model		Nilotinib SNEDDS	Nilotinib sSNEDDS
Zero-order	R^2	0.9895	0.9712
	n	0.1097	0.1302
First-order	R^2	0.9879	0.9698
	n	−0.00082	−0.0013
Higuchi	R^2	0.9413	0.9742
	n	2.96	3.6
Korsmeyer–Peppas	R^2	0.9948	0.9972
	n	0.8518	0.7723

Table 5. Stability Data of the Optimized SNEDDS (S3) Under Long-term (4 °C ± 1 °C and 25 °C ± 2 °C for 6 Months) and Accelerated (40 °C ± 2 °C/75 ± 5% RH for 3 Months) Storage Conditions.

	Mean Diameter (nm)			Zeta Potential			PDI		
Temperature (°C)	Months								
	0	3	6	0	3	6	0	3	6
40 °C/75% RH	105.56 ± 4.12	117.32 ± 5.12	–	−26.9 ± 1.8	−24.38 ± 1.6	–	0.060 ± 0.005	0.093 ± 0.005	–
4 ± 1 °C	105.56 ± 4.12	109.43 ± 3.26	111.78 ± 3.01	−26.9 ± 1.8	−25.8 ± 2.0	−25.6 ± 2.1	0.060 ± 0.005	0.074 ± 0.005	0.082 ± 0.005
25 ± 2 °C	105.56 ± 4.12	113.56 ± 3.48	116.92 ± 2.76	−26.9 ± 1.8	−25.1 ± 2.4	−24.8 ± 2.3	0.060 ± 0.005	0.086 ± 0.005	0.096 ± 0.005

Note: All values are expressed as mean ± SD (n = 3), no evidence of phase separation, creaming, or precipitation was observed throughout the study.

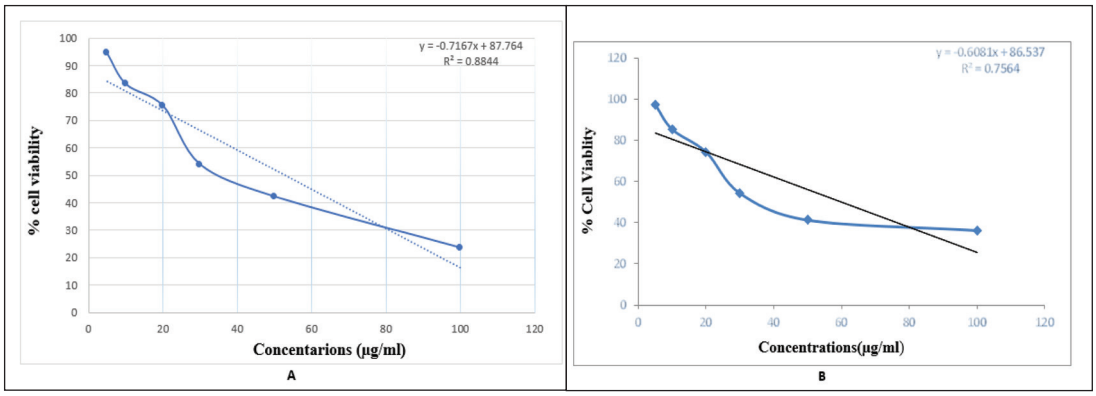

Figure 7. Cytotoxicity on K562 Cell Line. (A) Pure Drug (B) Test Formulation.

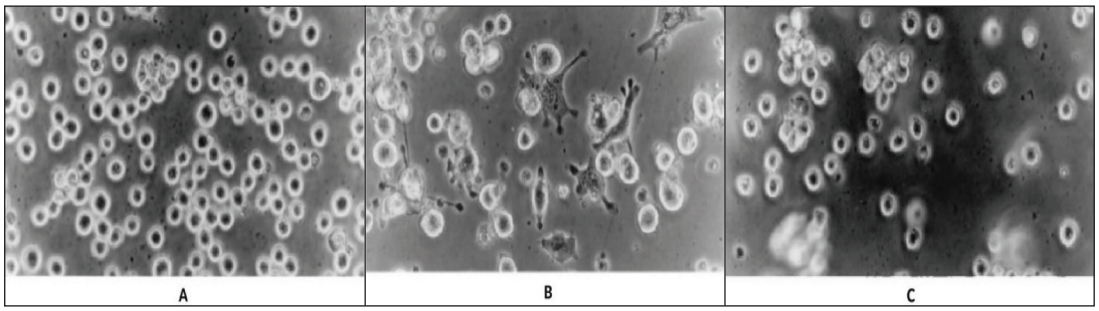

Figure 8. Morphological Changes of K562 Cancer Cells when Treated with (A) Control (Vehicle), (B) Pure Nilotinib, and (C) Nilotinib Test Formulation.

nilotinib test formulation in K562 cells, confirming their cytotoxic potential (Figure 7). The pure drug exhibited an IC_{50} of 72.45 µg/mL, whereas the test formulation showed an IC_{50} of 60.08 µg/mL, indicating enhanced antiproliferative activity. At lower concentrations (5–10 µg/mL), both formulations maintained high cell viability (>85%), while a marked reduction was observed at higher concentrations. At 100 µg/mL, the test formulation reduced cell viability to 23.53% ± 2.24%, compared with 36.25% ± 1.32% for the pure drug. The improved cytotoxicity of the formulation may be attributed to enhanced solubilization, increased cellular uptake, and sustained drug availability, consistent with the advantages of SNEDDS-based delivery systems.

Morphological examination (Figure 8) further supported these findings, showing pronounced cellular shrinkage and loss of membrane integrity in treated cells compared to controls. Importantly, the formulation components themselves exhibited no intrinsic cytotoxicity, confirming their biocompatibility. Overall, the results demonstrate that the optimized nilotinib formulation retains and slightly enhances the drug's anticancer activity while maintaining acceptable cell compatibility at lower concentrations. These findings support the development of an SNEDDS/sSNEDDS system to improve the therapeutic performance of nilotinib through enhanced delivery without compromising safety.

Conclusion

An sSNEDDS for nilotinib was successfully developed using an optimized liquid SNEDDS composed of castor oil, Kolliphor® EL, and propylene glycol. The Box–Behnken optimization predicted an optimized SNEDDS with a droplet size of 105.87 nm, a PDI of 0.069, and an EE% of 87.23%. Following solidification, the optimized sSNEDDS exhibited a particle size of 83.64 ± 3.12 nm, a PDI of 0.07 ± 0.005, and a zeta potential of −21.7 ± 1.5 mV. Stability studies confirmed the robustness of the formulation, while HPMC K4M effectively maintained drug supersaturation. Solid-state characterization demonstrated that nilotinib was present predominantly in an amorphous form, contributing to enhanced dissolution. Furthermore, the optimized sSNEDDS exhibited improved in vitro drug release and cytotoxic activity (IC_{50} = 60.08 µg/mL), indicating that this formulation is a promising strategy for improving the solubility, dissolution, stability, and therapeutic performance of poorly water-soluble antineoplastic agents.

Future Perspectives

Lipid-based nanoemulsion systems, such as self-emulsifying formulations, spontaneously form transparent nanoemulsions upon mild agitation in the gastrointestinal tract. In contrast to preformed nanoemulsions, these systems offer enhanced physical stability, ease of unit-dose encapsulation, improved patient compliance, and superior dissolution and oral bioavailability by facilitating efficient drug solubilization and permeability.

Acknowledgement

We gratefully acknowledge the management of Vels Institute of Science, Technology, and Advanced Studies for providing the necessary facilities and support that enabled the successful completion of this research.

Authors' Contribution

All authors made substantial contributions to conception and design, acquisition of data, or analysis and interpretation of data; took part in drafting the article or revising it critically for important intellectual content; agreed to submit to the current journal; gave final approval of the version to be published; and agreed to be accountable for all aspects of the work. All the authors are eligible to be authors as per the International Committee of Medical Journal Editors' requirements/guidelines.

Consent to Participate

Not applicable.

Consent for Publication

This work is original and not published or under consideration in any other journal.

Data Availability Statement

All the data are available with the authors and shall be provided upon request.

Declaration of Conflicting Interests

The authors declared no potential conflicts of interest with respect to the research, authorship, and/or publication of this article.

Ethical Approval

This study does not involve experiments on animals or human subjects.

Funding

The authors received no financial support for the research, authorship, and/or publication of this article.

Informed Consent

Not applicable.

Use of Artificial Intelligence-assisted Tools

The authors confirm that artificial intelligence (AI) tools (ChatGPT, OpenAI) were used solely for language editing, grammar correction, and improving clarity of the manuscript. All scientific content, data interpretation, and conclusions were developed and verified by the authors. The AI-generated text was carefully reviewed, edited, and validated to ensure accuracy, originality, and compliance with journal standards.

ORCID iDs

Vyshali Parigela https://orcid.org/0009-0005-1541-9984
Vijayalakshmi Arumugam https://orcid.org/0000-0002-8090-7248

References

1. Alves R, Gonçalves AC, Rutella S, et al. Resistance to tyrosine kinase inhibitors in chronic myeloid leukemia—from molecular mechanisms to clinical relevance. *Cancers (Basel)* 2021; 13(19): 4820.
2. Jabbour E, Kantarjian H and Cortes J. Use of second- and third-generation tyrosine kinase inhibitors in the treatment of chronic myeloid leukemia: an evolving treatment paradigm. *Clin Lymphoma Myeloma Leuk* 2015; 15(6): 323–334.
3. Ali MA. Chronic myeloid leukemia in the era of tyrosine kinase inhibitors: An evolving paradigm of molecularly targeted therapy. *Mol Diagn Ther* 2016; 20(4): 315–333.
4. National Center for Biotechnology Information. PubChem Compound Summary for CID 644241, Nilotinib. https://pubchem.ncbi.nlm.nih.gov/compound/Nilotinib (2025, accessed 14 May 2025).
5. Khivansara R, Jadhav S, Borkar M, et al. A concise review on analytical methods for determination of nilotinib. *Curr Anal Chem* 2023; 19(7): 513–530.

6. Tanaka C, Yin OQP, Sethuraman V, et al. Clinical pharmacokinetics of the BCR-ABL tyrosine kinase inhibitor nilotinib. *Clin Pharmacol Ther* 2010; 87(2): 197–203.
7. Zhu S, Yu R, Qian G, et al. A supersaturating drug delivery system to enhance the oral bioavailability of nilotinib. *J Drug Deliv Sci Technol* 2022; 68: 103038.
8. Colombo S, Brisander M, Haglöf J, et al. Matrix effects in nilotinib formulations with pH-responsive polymer produced by carbon dioxide-mediated precipitation. *Int J Pharm* 2015; 494(1): 205–217.
9. Ananthula HK, Parker S, Touchette E, et al. Preclinical pharmacokinetic evaluation to facilitate repurposing of tyrosine kinase inhibitors nilotinib and imatinib as antiviral agents. *BMC Pharmacol Toxicol* 2018; 19: 56.
10. Xia B, Heimbach T, He H, et al. Nilotinib preclinical pharmacokinetics and practical application toward clinical projections of oral absorption and systemic availability. *Biopharm Drug Dispos* 2012; 33(9): 536–549.
11. Hartmann JT, Haap M, Kopp HG, et al. Tyrosine kinase inhibitors: A review on pharmacology, metabolism and side effects. *Curr Drug Metab* 2009; 10(5): 470–481.
12. Tian X, Zhang H, Heimbach T, et al. Clinical pharmacokinetic and pharmacodynamic overview of nilotinib, a selective tyrosine kinase inhibitor. *J Clin Pharmacol* 2018; 58(12): 1533–1540.
13. Duckett DR, Cameron MD. Metabolism considerations for kinase inhibitors in cancer treatment. *Expert Opin Drug Metab Toxicol*. 2010;6(10):1175–1193.
14. Deininger MW. Nilotinib. *Clin Cancer Res* 2008; 14(13): 4027–4031.
15. Rix U, Hantschel O, Dürnberger G, et al. Chemical proteomic profiles of the BCR-ABL inhibitors imatinib, nilotinib, and dasatinib reveal novel kinase and nonkinase targets. *Blood* 2007; 110(12): 4055–4063.
16. Weisberg E, Manley P, Mestan J, et al. AMN107 (nilotinib): A novel and selective inhibitor of BCR-ABL. *Br J Cancer* 2006; 94(12): 1765–1769.
17. Zakkula A, Gabani BB, Jairam RK, et al. Preparation and optimization of nilotinib self-micro-emulsifying drug delivery systems to enhance oral bioavailability. *Drug Dev Ind Pharm* 2020; 46(3): 498–504.
18. Herbrink M, Nuijen B, Schellens JH, et al. Variability in bioavailability of small molecular tyrosine kinase inhibitors. *Cancer Treat Rev* 2015; 41(5): 412–422.
19. Mathias NR, Xu Y, Patel D, et al. Assessing the risk of pH-dependent absorption for new molecular entities: A novel in vitro dissolution test, physicochemical analysis, and risk assessment strategy. *Mol Pharm* 2013; 10(11): 4063–4073.
20. Salawi A. Self-emulsifying drug delivery systems: A novel approach to deliver drugs. *Drug Deliv* 2022; 29(1): 1811–1823.
21. Gao P and Morozowich W. Development of supersaturable self-emulsifying drug delivery system formulations for improving the oral absorption of poorly soluble drugs. *Expert Opin Drug Deliv* 2006; 3(1): 97–110.
22. Wang L, Dong J, Chen J, et al. Design and optimization of a new self-nanoemulsifying drug delivery system. *J Colloid Interface Sci* 2009; 330(2): 443–448.
23. Gupta S, Chavhan S and Sawant K. Self-nanoemulsifying drug delivery system for adefovir dipivoxil: Design, characterization, in vitro and ex vivo evaluation. *Colloids Surf A Physicochem Eng Asp* 2011; 392: 145–155.
24. Craig DQM, Barker SA, Banning D, et al. An investigation into the mechanisms of self-emulsification using particle size analysis and low frequency dielectric spectroscopy. *Int J Pharm* 1995; 114: 103–110.
25. Box GEP, Behnken DW. Some new three level designs for the study of quantitative variables. *Technometrics*. 1960;2(4): 455–475. doi:10.1080/00401706.1960.10489912.
26. Shivakumar HN, Patel PB, Desai BG, Ashok P, Arulmozhi S. Design and statistical optimization of glipizide loaded lipospheres using response surface methodology. *Acta Pharmaceutica*. 2007; 57(3): 269–285. DOI: 10.2478/v10007-007-0022-8.
27. Nazzal S, Khan MA. Response surface methodology for the optimization of ubiquinone self-nanoemulsified drug delivery system. *AAPS PharmSciTech*. 2002; 3(1): E3. DOI: 10.1208/pt030103.
28. Tran TH, Guo Y, Song D, et al. Quercetin-containing self-nanoemulsifying drug delivery system for improving oral bioavailability. *J Pharm Sci* 2014; 103(3): 840–852.
29. Zhang P, Liu Y, Feng N, et al. Preparation and evaluation of self-microemulsifying drug delivery system of oridonin. *Int J Pharm* 2008; 355: 269–276.
30. Bannow J, Yorulmaz Y, Löbmann K, Müllertz A, Rades T. Improving the drug load and in vitro performance of supersaturated self-nanoemulsifying drug delivery systems (super-SNEDDS) using polymeric precipitation inhibitors. *Int J Pharm*. 2020;574:118906. doi:10.1016/j.ijpharm.2019.118906
31. Xiao L, Yi T. Mechanisms of hydroxypropyl methylcellulose for the precipitation inhibitor of supersaturatable self-emulsifying drug delivery systems. *Yaoxue Xuebao*. 2013;48(5):767–772.